LDA++ approach to the electronic structure of magnets: correlation effects in iron

1999 J. Phys.: Condens. Matter 11 1037

(http://iopscience.iop.org/0953-8984/11/4/011)

J. Phys.: Condens. Matter **11** (1999) 1037–1048. Printed in the UK PII: S0953-8984(99)96712-7

LDA++ approach to the electronic structure of magnets: correlation effects in iron

M I Katsnelson† and A I Lichtenstein‡

† Institute of Metal Physics, 620219 Ekaterinburg, Russia
‡ Forschungszentrum Jülich, 52425 Jülich, Germany

Received 11 August 1998

Abstract. A novel approach to the investigation of correlation effects in the electronic structure of magnetic crystals which takes into account a frequency dependence of the self-energy (the so-called 'LDA++ approach') is developed. The fluctuation-exchange approximation is generalized to the spin-polarized multi-band case and a local version of it is proposed. As an example, we calculate the electronic quasiparticle spectrum of ferromagnetic iron. It is shown that the Fermi-liquid description of the bands near the Fermi level is reasonable, while the quasiparticle states beyond approximately the 1 eV range are strongly damped, in agreement with photoemission data. The result of the spin-polarized thermoemission experiment is explained satisfactorily. The problem of satellite structure is discussed.

1. Introduction

The description of the correlation effects in the electronic structure and magnetism of iron-group metals is still far from being a definitive picture and continues to attract interest (see, e.g., [1–4] and references therein). Despite the many attempts to remedy this, the situation is still unclear both theoretically and experimentally. For example, there is no agreement as regards whether a 5 eV satellite is present in the photoemission spectrum of iron [5, 6], or whether there is a local spin splitting above the Curie temperature of nickel [7]. The experimental data on the absence of spin polarization in the thermoemission from caesiated iron [8] are still not understood completely [9]. On the theoretical side, different approaches such as the second-order perturbation theory [3, 10], the three-body Faddeev approximation [11], and the moment expansion method [12] have been used. Unfortunately, the conditions of applicability of these schemes are not clear. Recently, we investigated different approximations to the LDA-based correlated electronic structure of crystals using a local self-energy [13] (the so-called 'LDA++' approach) and argued that for moderately strong correlations (such as are encountered in the case of iron-group metals) one of the most efficient approaches would be to use the fluctuation-exchange (FLEX) approximation of Bickers and Scalapino [14]. Here we generalize the LDA++ approach [13] to the spin-polarized case and present some results for the quasiparticle spectrum of ferromagnetic iron.

2. The spin-polarized multi-band FLEX approximation

Let us start with the general many-body Hamiltonian for crystal in the LDA + U scheme [15]:

$$H = H_t + H_U \tag{1}$$

0953-8984/99/041037+12$19.50

where

$$H_t = \sum_{\lambda\lambda'\sigma} t_{\lambda\lambda'} c^+_{\lambda\sigma} c_{\lambda'\sigma}$$
$$H_U = \frac{1}{2} \sum_{\{\lambda_i\}\sigma\sigma'} \langle \lambda_1\lambda_2 \,|v|\, \lambda'_1\lambda'_2\rangle c^+_{\lambda_1\sigma} c^+_{\lambda_2\sigma'} c_{\lambda'_2\sigma'} c_{\lambda'_1\sigma}$$

where the $\lambda = im$ are the site-number (i) and orbital (m) quantum numbers; $\sigma = \uparrow, \downarrow$ is the spin projection; c^+, c are the Fermi creation and annihilation operators; H_t is the effective single-particle Hamiltonian obtained from the LDA, corrected for double counting of average interactions among correlated electrons [13,15]; and the Coulomb matrix elements are defined in the standard way:

$$\langle 12 \,|v|\, 34\rangle = \int \mathrm{d}\boldsymbol{r}\, \mathrm{d}\boldsymbol{r}'\, \psi^*_1(\boldsymbol{r})\psi^*_2(\boldsymbol{r}')v(\boldsymbol{r}-\boldsymbol{r}')\psi_3(\boldsymbol{r})\psi_4(\boldsymbol{r}') \tag{2}$$

where we define for brevity $\lambda_1 \equiv 1$ etc. Following Bickers and Scalapino [14], we introduce the pairwise operators corresponding to different channels, namely:

(i) the particle–hole density:

$$d_{12} = \frac{1}{\sqrt{2}}(c^+_{1\uparrow}c_{2\uparrow} + c^+_{1\downarrow}c_{2\downarrow})$$

(ii) the particle–hole magnetic channel:

$$m^0_{12} = \frac{1}{\sqrt{2}}(c^+_{1\uparrow}c_{2\uparrow} - c^+_{1\downarrow}c_{2\downarrow})$$
$$m^+_{12} = c^+_{1\uparrow}c_{2\downarrow}$$
$$m^-_{12} = c^+_{1\downarrow}c_{2\uparrow}$$

(iii) the particle–particle singlet channel:

$$s_{12} = \frac{1}{\sqrt{2}}(c_{1\downarrow}c_{2\uparrow} - c_{1\uparrow}c_{2\downarrow})$$
$$\bar{s}_{12} = \frac{1}{\sqrt{2}}(c^+_{1\uparrow}c^+_{2\downarrow} - c^+_{1\downarrow}c^+_{2\uparrow})$$

(iv) the particle–particle triplet channel:

$$t^0_{12} = \frac{1}{\sqrt{2}}(c_{1\downarrow}c_{2\uparrow} + c_{1\uparrow}c_{2\downarrow})$$
$$\bar{t}^0_{12} = \frac{1}{\sqrt{2}}(c^+_{1\uparrow}c^+_{2\downarrow} + c^+_{1\downarrow}c^+_{2\uparrow})$$
$$t^\pm_{12} = c_{1\uparrow,\downarrow}c_{2\downarrow,\uparrow}$$
$$\bar{t}^\pm_{12} = c^+_{1\uparrow,\downarrow}c^+_{2\downarrow,\uparrow}.$$

The bare-vertex matrices corresponding to the different channels are defined as follows:

$$U^d_{12,34} = 2\langle 13 \,|v|\, 24\rangle - \langle 13 \,|v|\, 42\rangle$$
$$U^m_{12,34} = -\langle 13 \,|v|\, 42\rangle$$
$$U^s_{12,34} = \frac{1}{2}\left[\langle 12 \,|v|\, 34\rangle + \langle 12 \,|v|\, 43\rangle\right] \tag{3}$$
$$U^t_{12,34} = \frac{1}{2}\left[\langle 12 \,|v|\, 34\rangle - \langle 12 \,|v|\, 43\rangle\right].$$

Now we can rewrite the interaction part of the Hamiltonian of equation (1) in two equivalent forms, corresponding to the particle–hole and the particle–particle channels:

$$H_U = \frac{1}{2}\,\mathrm{Tr}\left\{ d * U^d * d + \sum_{\alpha=0,\pm} m^\alpha * U^m * m^{-\alpha} \right\}$$

$$H_U = \frac{1}{2}\,\mathrm{Tr}\left\{ \bar{s} * U^s * s + \sum_{\alpha=0,\pm} \bar{t}^\alpha * U^t * t^\alpha \right\}$$

where $*$ means the matrix product; e.g.,

$$(U^d * d)_{12} = \sum_{34} U^d_{12,34} d_{34}$$

$$(d * U^d)_{12} = \sum_{34} d_{34} U^d_{34,12}.$$

Then we may repeat the usual derivation of the FLEX equations for single-band [14] and multi-band [13, 16] cases, taking into account the spin dependence of the Green function $G^\sigma_{\lambda\lambda'}$:

$$G^\sigma_{12}(\tau) = -\left\langle T_\tau c_{1\sigma}(\tau) c^+_{2\sigma}(0) \right\rangle.$$

For finite temperature ($T > 0$), the FLEX equations have a 'local form' in the Matsubara frequency ($\mathrm{i}\omega_n$) or imaginary-time (τ) space (where $\omega_n = (2n+1)\pi T$, $n = 0, \pm 1, \ldots$), and it is very efficient to use the fast Fourier transforms (FFT) with periodic boundary conditions [13, 14]. The time and frequency spaces are connected by

$$G^\sigma_{\lambda\lambda'}(\mathrm{i}\omega_n) = \int_0^{1/T} \mathrm{e}^{\mathrm{i}\omega_n \tau} G^\sigma_{\lambda\lambda'}(\tau)\,\mathrm{d}\tau$$

$$G^\sigma_{\lambda\lambda'}(\tau) = T \sum_{\omega_n} \mathrm{e}^{-\mathrm{i}\omega_n \tau} G^\sigma_{\lambda\lambda'}(\mathrm{i}\omega_n)$$

and we will try to retain this dual $\mathrm{i}\omega$–τ notation to stress the numerical implementation of this LDA++ scheme.

An unusual feature of the spin-polarized multi-band FLEX scheme is the mixing of m^0- and d-channels (as well as s- and t^0-channels) which is related to the non-zero value of the appropriate correlator; for example,

$$\left\langle\!\left\langle d_{12} m^0_{34} \right\rangle\!\right\rangle_c = \frac{1}{2}\left\langle\!\left\langle (c^+_{1\uparrow} c_{2\uparrow} + c^+_{1\downarrow} c_{2\downarrow})(c^+_{3\uparrow} c_{4\uparrow} - c^+_{3\downarrow} c_{4\downarrow}) \right\rangle\!\right\rangle_c = -\frac{1}{2}\left\{ G^\uparrow_{23} G^\uparrow_{41} - G^\downarrow_{23} G^\downarrow_{41} \right\} \tag{4}$$

where subscript c indicates a connected part of the correlator (cf. [14]). As a result, we have the following expression for the effective-transverse-susceptibility matrix:

$$\chi^{+-}(\mathrm{i}\omega) = \left[1 + U^m * \Gamma^{\uparrow\downarrow}(\mathrm{i}\omega)\right]^{-1} * \Gamma^{\uparrow\downarrow}(\mathrm{i}\omega) \tag{5}$$

where

$$\Gamma^{\sigma\sigma'}_{12,34}(\tau) = -G^\sigma_{23}(\tau) G^{\sigma'}_{41}(-\tau) \tag{6}$$

is an 'empty loop' and $\Gamma(\mathrm{i}\omega)$ is its Fourier transform. The corresponding longitudinal susceptibility matrix has a more complicated form:

$$\chi^{\parallel}(\mathrm{i}\omega) = \left[1 + U^{\parallel}_{ph} * \chi^{\parallel}_0(\mathrm{i}\omega)\right]^{-1} * \chi^{\parallel}_0(\mathrm{i}\omega) \tag{7}$$

where we have introduced the supermatrix of p–h interactions:

$$U^{\parallel}_{ph} = \begin{pmatrix} U^d & 0 \\ 0 & U^m \end{pmatrix}$$

and the matrix of bare longitudinal susceptibility:

$$\chi_0^{\parallel} = \frac{1}{2}\begin{pmatrix} \Gamma^{\uparrow\uparrow} + \Gamma^{\downarrow\downarrow} & \Gamma^{\uparrow\uparrow} - \Gamma^{\downarrow\downarrow} \\ \Gamma^{\uparrow\uparrow} - \Gamma^{\downarrow\downarrow} & \Gamma^{\uparrow\uparrow} + \Gamma^{\downarrow\downarrow} \end{pmatrix} \tag{8}$$

in the dd-, dm^0-, m^0d-, and m^0m^0-channels ($d, m^0 = 1, 2$ in the supermatrix indices). Similarly, for the p–p channel we have

$$\begin{aligned} R^{\pm}(\mathrm{i}\omega) &= \left[1 + U^t * R_0^{\pm}(\mathrm{i}\omega)\right]^{-1} * R_0^{\pm}(\mathrm{i}\omega) \\ R^{\parallel}(\mathrm{i}\omega) &= \left[1 + U_{pp}^{\parallel} * R_0^{\parallel}(\mathrm{i}\omega)\right]^{-1} * R_0^{\parallel}(\mathrm{i}\omega) \end{aligned} \tag{9}$$

where the supermatrix of p–p interactions is defined as follows:

$$U_{pp}^{\parallel} = \begin{pmatrix} U^s & 0 \\ 0 & U^t \end{pmatrix}$$

and the bare p–p susceptibilities are

$$\begin{aligned} \left[R_0^{\pm}(\tau)\right]_{12,34} &= \frac{1}{2}\left[G_{14}^{\uparrow,\downarrow}(\tau)G_{23}^{\uparrow,\downarrow}(\tau) - G_{13}^{\uparrow,\downarrow}(\tau)G_{24}^{\uparrow,\downarrow}(\tau)\right] \\ R_0^{\parallel} &= \begin{pmatrix} R_0^{ss} & R_0^{st} \\ R_0^{ts} & R_0^{tt} \end{pmatrix} \end{aligned} \tag{10}$$

where

$$\Pi_{12,34}^{\sigma\sigma'}(\tau) = G_{23}^{\sigma}(\tau)G_{14}^{\sigma'}(\tau)$$

and

$$\begin{aligned} \left[R_0^{ss}\right]_{12,34} &= \frac{1}{4}\left[\Pi_{12,34}^{\uparrow\downarrow} + \Pi_{21,34}^{\uparrow\downarrow} + \Pi_{21,34}^{\downarrow\uparrow} + \Pi_{12,34}^{\downarrow\uparrow}\right] \\ \left[R_0^{st}\right]_{12,34} &= \frac{1}{4}\left[\Pi_{12,34}^{\uparrow\downarrow} + \Pi_{21,34}^{\uparrow\downarrow} - \Pi_{21,34}^{\downarrow\uparrow} - \Pi_{12,34}^{\downarrow\uparrow}\right] \\ \left[R_0^{ts}\right]_{12,34} &= \frac{1}{4}\left[\Pi_{12,34}^{\uparrow\downarrow} - \Pi_{21,34}^{\uparrow\downarrow} + \Pi_{21,34}^{\downarrow\uparrow} - \Pi_{12,34}^{\downarrow\uparrow}\right] \\ \left[R_0^{tt}\right]_{12,34} &= \frac{1}{4}\left[\Pi_{12,34}^{\uparrow\downarrow} - \Pi_{21,34}^{\uparrow\downarrow} - \Pi_{21,34}^{\downarrow\uparrow} + \Pi_{12,34}^{\downarrow\uparrow}\right]. \end{aligned} \tag{11}$$

In the FLEX approximation we can calculate the electronic self-energy in terms of the effective interactions in various channels:

$$\Sigma = \Sigma^{HF} + \Sigma^{(2)} + \Sigma^{(ph)} + \Sigma^{(pp)} \tag{12}$$

where the Hartree–Fock contribution is equal to

$$\Sigma_{12,\sigma}^{HF} = \sum_{34}\left[\langle 13\,|v|\,24\rangle \sum_{\sigma'} n_{34}^{\sigma'} - \langle 13\,|v|\,42\rangle\, n_{34}^{\sigma}\right] \tag{13}$$

with the occupation matrix $n_{12}^{\sigma} = G_{21}^{\sigma}(\tau \to -0)$; this contribution to Σ is equivalent to the spin-polarized 'rotationally invariant' LDA + U method [17].

The second-order contribution in the spin-polarized case reads

$$\begin{aligned} \Sigma_{12,\sigma}^{(2)}(\tau) = &- \sum_{\{3-8\}} \langle 13\,|v|\,74\rangle\, G_{78}^{\sigma}(\tau) \\ &\times \left[\langle 85\,|v|\,26\rangle \sum_{\sigma'} G_{63}^{\sigma'}(\tau)G_{45}^{\sigma'}(-\tau) - \langle 85\,|v|\,62\rangle\, G_{63}^{\sigma}(\tau)G_{45}^{\sigma}(-\tau)\right] \end{aligned} \tag{14}$$

and the higher-order particle–hole contribution reads

$$\Sigma_{12,\sigma}^{(ph)}(\tau) = \sum_{34,\sigma'} W_{13,42}^{\sigma\sigma'}(\tau)G_{34}^{\sigma'}(\tau) \tag{15}$$

with the p–h fluctuation potential matrix

$$W^{\sigma\sigma'}(\mathrm{i}\omega) = \begin{bmatrix} W^{\uparrow\uparrow}(\mathrm{i}\omega) & W^{\uparrow\downarrow}(\mathrm{i}\omega) \\ W^{\downarrow\uparrow}(\mathrm{i}\omega) & W^{\downarrow\downarrow}(\mathrm{i}\omega) \end{bmatrix} \tag{16}$$

where the spin-dependent effective potentials are defined as follows:

$$\begin{aligned} W^{\uparrow\uparrow} &= \frac{1}{2}\{U^d * [\chi^{dd} - \chi_0^{dd}] * U^d + U^m * [\chi^{mm} - \chi_0^{mm}] * U^m \\ &\quad + U^d * [\chi^{dm} - \chi_0^{dm}] * U^m + U^m * [\chi^{md} - \chi_0^{md}] * U^d\} \\ W^{\downarrow\downarrow} &= \frac{1}{2}\{U^d * [\chi^{dd} - \chi_0^{dd}] * U^d + U^m * [\chi^{mm} - \chi_0^{mm}] * U^m \\ &\quad - U^d * [\chi^{dm} - \chi_0^{dm}] * U^m - U^m * [\chi^{md} - \chi_0^{md}] * U^d\} \\ W^{\uparrow\downarrow} &= U^m * [\chi^{+-} - \chi_0^{+-}] * U^m \\ W^{\downarrow\uparrow} &= U^m * [\chi^{-+} - \chi_0^{-+}] * U^m. \end{aligned}$$

Finally, the higher-order particle–particle contribution corresponds to

$$\Sigma^{(pp)}_{12,\sigma}(\tau) = -\sum_{34,\sigma'} T^{\sigma\sigma'}_{13,42}(\tau) G^{\sigma'}_{43}(\tau)$$

with the p–p fluctuation potential matrix

$$T^{\sigma\sigma'}(\mathrm{i}\omega) = \left[\begin{pmatrix} T^{\uparrow\uparrow}(-\mathrm{i}\omega) & T^{\uparrow\downarrow}(-\mathrm{i}\omega) \\ T^{\downarrow\uparrow}(-\mathrm{i}\omega) & T^{\downarrow\downarrow}(-\mathrm{i}\omega) \end{pmatrix}\right] \tag{17}$$

defined in terms of the spin-dependent p–p effective potentials:

$$\begin{aligned} T^{\uparrow\downarrow} &= U^s * [R^{ss} - R_0^{ss}] * U^s + U^t * [R^{tt} - R_0^{tt}] * U^r \\ &\quad + U^s * [R^{st} - R_0^{st}] * U^t + U^t * [R^{ts} - R_0^{ts}] * U^s \\ T^{\downarrow\uparrow} &= U^s * [R^{ss} - R_0^{ss}] * U^s + U^t * [R^{tt} - R_0^{tt}] * U^r \\ &\quad - U^s * [R^{st} - R_0^{st}] * U^t - U^t * [R^{ts} - R_0^{ts}] * U^s \\ T^{\uparrow\uparrow} &= U^t * [R^{+} - R_0^{+}] * U^t \\ T^{\downarrow\downarrow} &= U^t * [R^{-} - R_0^{-}] * U^t. \end{aligned}$$

Note that for both p–h and p–p channels, the effective interactions, according to equations (16) and (17), are non-diagonal matrices in spin space, in contrast to the case for any mean-field approximation like the LSDA.

3. Local approximation

The consideration of the full non-local FLEX self-energy $\Sigma_{ij}(\mathrm{i}\omega)$ (or the momentum-dependent Fourier transform $\Sigma(\boldsymbol{k}, \mathrm{i}\omega)$) in the framework of realistic multi-band calculations encounters significant computational difficulties [16]. On the other hand, the best local approximation, which corresponds to the so-called dynamical mean-field theory (DMFT) [19], appeared to be very effective for the calculation of the electron spectra of strongly correlated systems. Therefore, it is reasonable to combine the FLEX approximation with DMFT rather than just neglecting the momentum dependence in FLEX equations. In this respect, we will take into account only on-site (Hubbard) interactions, so all of the bare vertices (equation (3)) are diagonal in the site index i but are matrices in the orbital indices $\{m\}$. We believe that this self-consistent local FLEX approximation partly accounts for 'vertex corrections' (due to the difference of G and $\mathcal{G}_0$; see below) which are absent in the usual FLEX method. Moreover,

it is known that even a simple second-order approximation for the self-energy combined with the DMFT gives rather good results for the description of correlated systems—the Hubbard splitting, 'Kondo resonances', etc [19].

The DMFT procedure applied to the lattice is as follows: one needs to find a self-consistent solution of the functional equations

$$\mathcal{G}_0^{-1}(\mathrm{i}\omega) = G^{-1}(\mathrm{i}\omega) + \Sigma(\mathrm{i}\omega) \tag{18}$$

and

$$\Sigma = \Sigma[\mathcal{G}_0]$$

where

$$G(\mathrm{i}\omega) = \sum_{\boldsymbol{k}} [\mathrm{i}\omega + \mu - t(\boldsymbol{k}) - \Sigma(\mathrm{i}\omega)]^{-1} \tag{19}$$

is the matrix (in orbital and spin indices) of the local Green function, and Σ (equation (12)) is our spin-polarized multi-band FLEX solution which depends on the effective-media Green function $\mathcal{G}_0$.

We could further simplify the computational procedure by neglecting dynamical interaction in the p–p channel, since the most important fluctuations in itinerant-electron magnets are spin fluctuations in the p–h channel. We take into account static (of T-matrix type) renormalization of the effective interactions, replacing the bare matrix $U_{12,34} = \langle 12|v|34\rangle$ in equations (14) and (15) with the corresponding scattering T-matrix averaged over spins:

$$\overline{U} = [1 + U * \Pi_0(\mathrm{i}\omega = 0)]^{-1} * U$$

where $\Pi_0(\mathrm{i}\omega)$ is the Fourier transform of

$$\Pi^0_{12,34}(\tau) = \frac{1}{4}\sum_{\sigma\sigma'} G^{\sigma}_{13}(\tau) G^{\sigma'}_{24}(\tau).$$

In the case of the single-band Hubbard model, this approximation was found to be very reliable [18]. The effects of the spin dependence of the effective interaction matrix $\overline{U}$ will be considered elsewhere [20].

4. Computational results

We have started from the spin-polarized LSDA band structure of ferromagnetic iron within the TB-LMTO method [21] in the minimal s, p, d basis set and used numerical orthogonalization to find the H_t-part of our starting Hamiltonian. We take into account Coulomb interactions only between d states. The correct parametrization of the H_U-part is a serious problem. For example, first-principles estimations of the average Coulomb interactions (U) [3, 22] lead to unreasonably large values of the order of 5–6 eV, in comparison with experimental values of the U-parameter in the range 1–2 eV for iron [3]. Semiempirical analysis of the appropriate interaction value [23] gives $U \simeq 2.3$ eV. The difficulties as regards choosing the correct value of U are connected with complicated screening problems, definitions of orthogonal orbitals in the crystal, and contributions of the inter-site interactions. In the quasiatomic (spherical) approximation, the full U-matrix for the d shell is determined by the three parameters U, J, and δJ, or equivalently by effective Slater integrals F^0, F^2, and F^4 [13, 15]. For example, $U = F^0$, $J = (F^2 + F^4)/14$, and we use the simplest way of estimating δJ or F^4, keeping the ratio F^2/F^4 equal to its atomic value 0.625 [24]. The total Coulomb matrix in equation (1) is defined as

$$\langle m_1 m_2 \,|v|\, m_1' m_2' \rangle = \sum_k a_k(m_1, m_1', m_2, m_2') F^k$$

where $0 \leqslant k \leqslant 2l$ and

$$a_k(m_1, m_1', m_2, m_2') = \frac{4\pi}{2k+1} \sum_{q=-k}^{k} \langle lm_1|Y_{kq}|lm_1'\rangle \langle lm_2|Y_{kq}^*|lm_2'\rangle.$$

Note that the value of the intra-atomic (Hund) exchange interaction J is not sensitive to the screening, and is approximately equal to 0.9 eV in different estimations [22]. For the most important parameter U, which defines the bare-vertex matrix (equation (3)), we use the value $U = 2.3$ eV for most of our calculations, and discuss the dependences of the density of states (DOS) as functions of U. To calculate the spectral functions

$$A_\sigma(\boldsymbol{k}, E) = -\frac{1}{\pi} \mathrm{Tr}_L \, G_\sigma(\boldsymbol{k}, E + \mathrm{i}0)$$

and the DOS as their sums over the Brillouin zone, we first carried out analytical continuation for the matrix self-energy from the Matsubara frequencies to the real axis using the Padé approximation [25], and then numerically inverted the Green-function matrix as in equation (19) for each $\boldsymbol{k}$-point. In the self-consistent solution of the FLEX equations we used 1024 Matsubara frequencies and the FFT scheme with the energy cut-off at 100 eV. The sums over the irreducible Brillouin zone have been performed with 72 k-points for SCF iterations and with 1661 k-points for the final total density of states.

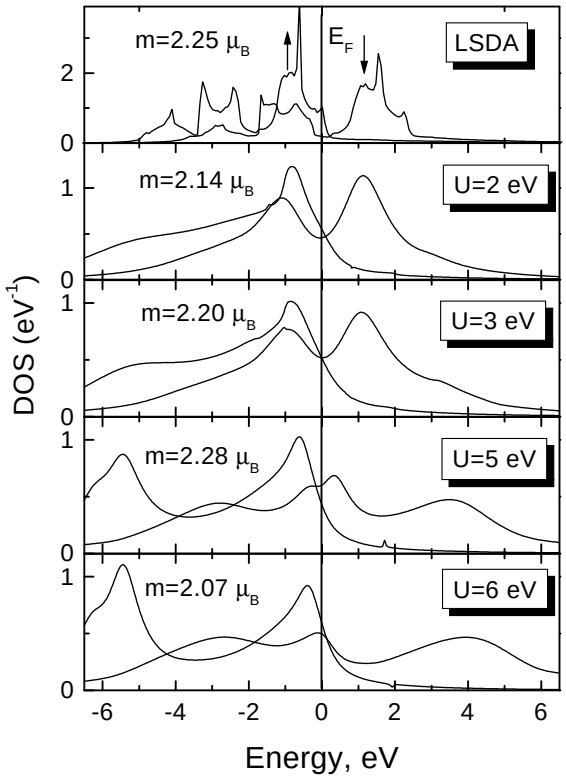

Figure 1. The spin-resolved density of d states and magnetic moments for ferromagnetic iron in the LSDA and the LDA++ calculations for different average Coulomb interactions with $J = 0.9$ eV and temperature $T = 1500$ K.

First we analyse the U-dependence of the electronic structure (figure 1). Keeping J, δJ fixed as described above, we vary the average U-parameter over the range from 2 to 6 eV. For

computational simplicity, a relatively high temperature value $T = 1500$ K was used. Note that the temperature in this approach is defined in terms of Matsubara frequencies. In contrast to the case for the standard LDA calculations at finite temperatures [26], we take into account the temperature dependence of the Bose degrees of freedom through the p–h susceptibilities. It is known [27] that this source of temperature dependence is the most important for itinerant-electron magnets. Although T is above $T_C^{\rm exp}$ (where $T_C^{\rm exp} = 1043$ K is the experimental value of the Curie temperature of iron), all of the DOS ($N_\uparrow(E)$, $N_\downarrow(E)$) curves in figure 1 show spin splitting. In principle, one could calculate T_C using the temperature dependence of the uniform spin susceptibility [19], but we have not done this yet. Nevertheless, we believe that this splitting in the DMFT is a manifestation of the existence of a local magnetic moment above T_C, and is not connected with long-range magnetic order. This spin splitting is a characteristic feature of local approximations, and reflects the Hubbard splitting in the one-band model [18]. The local spin splitting above the Curie temperature in iron is definitely observed in many experiments—e.g. optics and photoemission investigations (see, e.g., [4, 27] and references therein).

First of all, we see that the value of the total magnetic moment is weakly dependent on U, and is of the order of $2\mu_B$ for this temperature. The positions of the main peaks

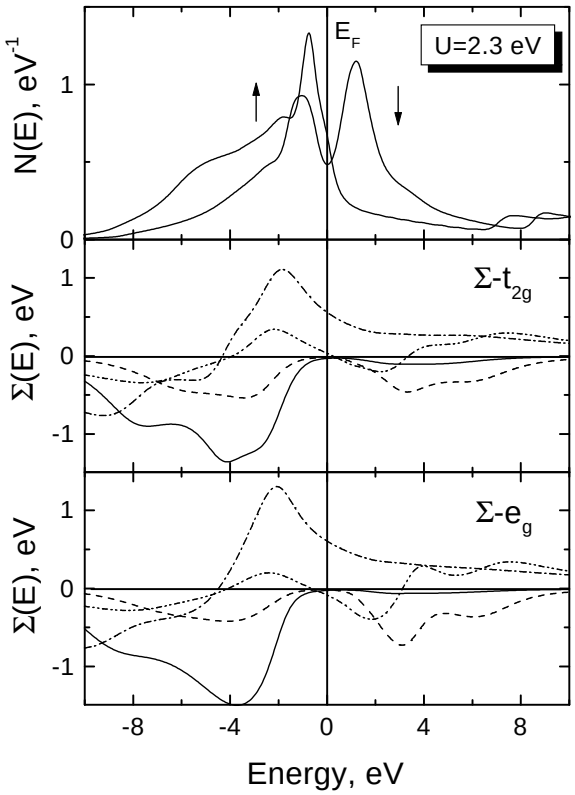

Figure 2. The total spin-polarized density of states and the d part of the self-energy for iron with $U = 2.3$ eV and $J = 0.9$ eV for the temperature $T = 750$ K. Two different self-energies for t_{2g} and e_g d states in the cubic crystal-field symmetry are presented and four different curves correspond to the imaginary part with spin up (full curve) and spin down (dashed curve) as well as real part with spin up (dashed–dotted curve) and spin down (dashed–double-dotted curve).

with respect to the Fermi energy roughly coincide with those in the LSDA up to $U = 2$ eV. Starting from $U = 3$ eV, satellites at $E \simeq -5$ eV appear as well as additional many-body structure at $E \simeq 4$ eV. Note that a weak satellite-like feature at $E \simeq -5$ eV was observed experimentally in [5], although it was not found in [6]. For $U \simeq 1$ eV, which is considered to be the 'experimental' value for iron [3], there are no noticeable manifestations of this satellite. The boundary values of U of the order of 2 eV with a weak shoulder probably correspond to the experimental situation best. For $U \simeq 5$–6 eV an essential part of the spectral density is related to the many-particle peaks corresponding to the upper and lower Hubbard bands, which is unrealistic for such moderately correlated substances as iron. At $U \simeq 6$ eV, the empty quasiparticle minority-spin peak goes below the Fermi level, which decreases the magnetic moment.

The depolarization of states near the Fermi level is another important correlation effect. The decrease of the ratio

$$P = [N_\uparrow(E_F) - N_\downarrow(E_F)]/[N_\uparrow(E_F) + N_\downarrow(E_F)]$$

is a typical sign of spin-polaron effects [4, 28]. In our approach, these effects are taken into account through the $W^{(ph)}_{\uparrow\downarrow}$ terms in the effective spin-polarized LDA++ potential.

The energy dependence of the self-energy in figure 2 shows characteristic features of moderately correlated systems. At low energies, $|E| < 1$ eV, we see a typical Fermi-liquid behaviour, $\mathrm{Im}\,\Sigma(E) \sim -E^2$, $\partial\,\mathrm{Re}\,\Sigma(E)/\partial E < 0$. At the same time, for the states beyond this interval within the d bands, the damping is rather large (of the order of 1 eV), so these states correspond to ill-defined quasiparticles, especially for occupied states. This is probably one of the most important conclusions of our calculations. Qualitatively, this had already been pointed out in reference [10] on the basis of model second-order perturbation theory calculations. We have shown that this is the case for a realistic quasiparticle structure of iron with a reasonable value of the Coulomb interaction parameter.

In view of the noticeable broadening of the quasiparticle states, a description of the computational results in terms of an effective band structure (determined, for example, from the maximum of the spectral density) would be incomplete. We present in figure 3 the *full*-spectral density $A_\sigma(\boldsymbol{k}, E)$, including both coherent and incoherent parts as a function of $\boldsymbol{k}$ and E. We see that in general the maxima of the spectral density (dark regions) coincide with the experimentally obtained band structure. However, for occupied majority-spin states at about -3 eV, the distribution of the spectral density is rather broad and the description of these states in terms of the quasiparticle dispersion is problematic. This conclusion is in complete quantitative agreement with the raw experimental data on the angle-resolved spin-polarized photoemission [29] with the broad non-dispersive second peak in the spin-up spectral function at around -3 eV.

5. Applications to spin-polarized thermoemission

One of the most unexpected results as regards the electronic structure of iron was obtained from the spin-polarized thermoemission for caesiated iron [8]. In this case the thermal current is determined by the states with the energy $W = 1.37$ eV above the Fermi level, which are in the region of the quasiparticle DOS peak for the minority spin. One could expect a strong negative spin polarization of the current (the polarization ratio P as estimated from the LSDA DOS is about -85%). More accurate estimation, which takes into account group velocities [9], gives the result $P = -34\%$ for the polarization ratio. Experimentally, it found to be zero within the experimental error.

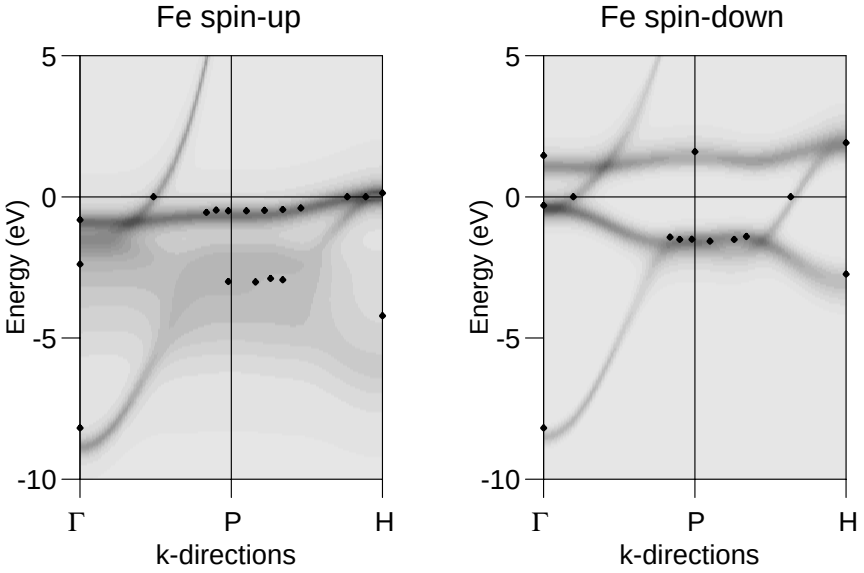

Figure 3. The spectral function of ferromagnetic iron for spin up (a) and spin down (b), and the two k-directions in the Brillouin zone, compared with the experimental angle-resolved photoemission and de Haas–van Alphen (at $E_F = 0$) points (from reference [3]).

To clarify the situation, we considered this effect on the basis of our LDA++ calculations. The current through the surface $x = 0$ in the spectral representation is

$$j_x = \sum_{\boldsymbol{k}} \mathrm{Tr}_{L\sigma} \left[\frac{\partial t(\boldsymbol{k})}{\partial k_x} \left\langle c^+_{\boldsymbol{k}} c_{\boldsymbol{k}} \right\rangle \right] = \sum_{\boldsymbol{k}} \mathrm{Tr}_{L\sigma} \left\{ \frac{\partial t(\boldsymbol{k})}{\partial k_x} \left[\int_{-\infty}^{\infty} \mathrm{d}E \; f(E) A(\boldsymbol{k}, E) \right] \right\} \tag{20}$$

where $\partial t(\boldsymbol{k})/\partial \boldsymbol{k} = \boldsymbol{V}_{\boldsymbol{k}}$ is the group velocity operator (the matrix in orbital indices), and $f(E)$ is the Fermi distribution function. Taking into account only electrons moving towards the surface ($k_x > 0$) and with the energy E above the barrier (W), the thermoemission current (cf. reference [9] for the case of non-interacting electrons) could be expressed as

$$j_x^T = \sum_{\boldsymbol{k}(k_x>0)} \int_W^{\infty} \mathrm{d}E \; f(E) \, \mathrm{Tr}_{L\sigma} \left\{ \left| \frac{\partial t(\boldsymbol{k})}{\partial k_x} \right| A(\boldsymbol{k}, E) \right\}. \tag{21}$$

Taking into account that $T \ll W$ and averaging over the surface orientations (experiments [8] were carried out for polycrystalline samples), we found the following approximate formula for the polarization:

$$P = \frac{I_\uparrow - I_\downarrow}{I_\uparrow + I_\downarrow} \tag{22}$$

where

$$I_\sigma = \sum_{i=x,y,z} \sum_{\boldsymbol{k}} \mathrm{Tr}_L \left\{ \left| \frac{\partial t(\boldsymbol{k})}{\partial k_i} \right| A_\sigma(\boldsymbol{k}, W) \right\}.$$

This was calculated using numerical differentiation of the $t(\boldsymbol{k})$ matrix and summing over 1661 $\boldsymbol{k}$-points in the irreducible part of the Brillouin zone. We obtained $P = -12\%$, which is to be

compared with the value of -34% obtained from LSDA calculations [9]. The decrease of P is not purely an effect of damping of the quasiparticle states, but is the result of rather complicated cancellations of s-, p-, and d-electron contributions. Therefore, one may conclude that there is no drastic discrepancy between the experimental results [8] and the theoretical description of the electronic structure of iron, in spite of the approximate character of our treatment of the thermoemission problem. For a more accurate description, one needs to consider the surface effects as well as the influence of the caesium layer on the electronic structure of iron according to the experimental conditions.

6. Conclusions

We have proposed a general scheme for investigation of the correlation effects in the quasiparticle band-structure calculations for itinerant-electron magnets. This approach is based on the combination of the dynamical mean-field theory and the fluctuation-exchange approximation. Application of the LDA++ method gives an adequate description of the quasiparticle electronic structure for ferromagnetic iron. The main correlation effects in the electron energy spectrum are the strong damping of the occupied states below 1 eV from the Fermi level E_F and the significant depolarization of the states in the vicinity of E_F. We obtained a reasonable agreement with different experimental spectral data (from spin-polarized photoemission and thermoemission). The method is rather universal, and can be applied to other magnetic systems, both ferromagnetic and antiferromagnetic.

Acknowledgments

Part of this work was carried out during the visit of one of the authors (MIK) to the Max Planck Institute of Physics for Complex Systems (Dresden). The work was also partially supported by the Russian Basic Research Foundation under grant 96-02-16000. We are grateful to O K Andersen, C Carbone, P Fulde, O Gunnarsson, G Kotliar, and A Georges for helpful discussions.

References

[1] Liebsch A 1979 *Phys. Rev. Lett.* **43** 1431
[2] Staunton J, Gyorffy B L, Pindor A J, Stocks G M and Winter H 1985 *J. Phys. F: Met. Phys.* **15** 1387
[3] Steiner M M, Albers R C and Sham L J 1992 *Phys. Rev.* B **45** 13 272
[4] Irkhin V Yu, Katsnelson M I and Trefilov A V 1993 *J. Phys.: Condens. Matter* **5** 8763
Vonsovsky S V, Katsnelson M I and Trefilov A V 1993 *Phys. Met. Metallogr.* **76** 247
Vonsovsky S V, Katsnelson M I and Trefilov A V 1993 *Phys. Met. Metallogr.* **76** 343
[5] Chanderis D, Lecante J and Petroff Y 1983 *Phys. Rev.* B **27** 2630
Gutierez A and Lopez M F 1997 *Phys. Rev.* B **56** 1111
[6] Kirby R E, Kisker B, King F K and Garwin E L 1985 *Solid State Commun.* **56** 425
[7] Greber T, Kreuntz T J and Osterwalder J 1997 *Phys. Rev. Lett.* **79** 4465
Sinkovich B, Tjeng L H, Brooks N B, Goedkoop J B, Hesper R, Pellegrin E, de Groot F M F, Altieri S, Hulbert S L, Shekel E and Sawatzky G A 1997 *Phys. Rev. Lett.* **79** 3510
[8] Vaterlaus A, Milani F and Meier F 1990 *Phys. Rev. Lett.* **65** 3041
[9] Monnier R, Steiner M M and Sham L J 1991 *Phys. Rev.* B **44** 13 678
[10] Treglia G, Ducastelle F and Spanjaard D 1982 *J. Physique* **43** 341
[11] Igarashi J 1983 *J. Phys. Soc. Japan* **52** 2827
Manghi F, Bellini V and Arcangeli C 1997 *Phys. Rev.* B **56** 7149
[12] Nolting W, Rex S and Mathi Jaya S 1987 *J. Phys.: Condens. Matter* **9** 1301
[13] Lichtenstein A I and Katsnelson M I 1998 *Phys. Rev.* B **57** 6884
[14] Bickers N E and Scalapino D J 1989 *Ann. Phys., NY* **193** 206

[15] Anisimov V I, Aryasetiawan F and Lichtenstein A I 1997 *J. Phys.: Condens. Matter* **9** 767
[16] Esirgen G and Bickers N E 1998 *Phys. Rev.* B **57** 5376
[17] Liechtenstein A I, Anisimov V I and Zaanen J 1995 *Phys. Rev.* B **52** R5467
[18] Fleck M, Liechtenstein A I, Oles A M, Hedin L and Anisimov V I 1998 *Phys. Rev. Lett.* **80** 2393
[19] Georges A, Kotliar G, Krauth W and Rozenberg M 1996 *Rev. Mod. Phys.* **68** 13
[20] Katsnelson M I and Lichtenstein A I 1999 to be published
[21] Andersen O K 1975 *Phys. Rev.* B **12** 3060
Krier G, Jepsen O, Burkhardt A and Andersen O K 1994 The TB-LMTO-ASA program *Preprint* Max Planck Institute of Solid State Research, Stuttgart
[22] Anisimov V I and Gunnarsson O 1991 *Phys. Rev.* B **43** 7570
[23] Oles A M and Stolhoff G 1984 *Phys. Rev.* B **29** 314
[24] Anisimov V I, Solovjev I V, Korotin M A, Czyzyk M T and Sawatzky G A 1993 *Phys. Rev.* B **48** 16 929
[25] Vidberg H J and Serene J W 1977 *J. Low Temp. Phys.* **29** 179
[26] Jarlborg T 1997 *Rep. Prog. Phys.* **60** 1305
[27] Moriya T 1985 *Spin Fluctuations in Itinerant Electron Magnetism* (Berlin: Springer)
[28] Irkhin V Yu and Katsnelson M I 1994 *Sov. Phys.–Usp.* **37** 659
[29] Kisker E, Schroeder K, Gudat T and Campagna M 1985 *Phys. Rev.* B **31** 329